Neuropsychopharmacology

ARTICLE

Aberrant triple-network connectivity patterns discriminate biotypes of first-episode medication-naive schizophrenia in two large independent cohorts

Sugai Liang[1,2], Qiang Wang[1], Andrew J. Greenshaw[3], Xiaojing Li[1], Wei Deng[1,2], Hongyan Ren[1], Chengcheng Zhang[1], Hua Yu[1], Wei Wei[1], Yamin Zhang[1], Mingli Li[1], Liansheng Zhao[1], Xiangdong Du[4], Yajing Meng[1], Xiaohong Ma[1], Chao-Gan Yan[5,6] and Tao Li[1,2]

Schizophrenia is a complex disorder associated with aberrant brain functional connectivity. This study aims to demonstrate the relation of heterogeneous symptomatology in this disorder to distinct brain connectivity patterns within the triple-network model. The study sample comprised 300 first-episode antipsychotic-naive patients with schizophrenia (FES) and 301 healthy controls (HCs). At baseline, resting-state functional magnetic resonance imaging data were captured for each participant, and concomitant neurocognitive functions were evaluated outside the scanner. Clinical information of 49 FES in the discovery dataset were reevaluated at a 6-week follow-up. Differential features between FES and HCs were selected from triple-network connectivity profiles. Cutting-edge unsupervised machine learning algorithms were used to define patient subtypes. Clinical and cognitive variables were compared between patient subgroups. Two FES subgroups with differing triple-network connectivity profiles were identified in the discovery dataset and confirmed in an independent hold-out cohort. One patient subgroup appearing to have more severe clinical symptoms was distinguished by salience network (SN)-centered hypoconnectivity, which was associated with greater impairments in sustained attention. The other subgroup exhibited hyperconnectivity and manifested greater deficits in cognitive flexibility. The SN-centered hypoconnectivity subgroup had more persistent negative symptoms at the 6-week follow-up than the hyperconnectivity subgroup. The present study illustrates that clinically relevant cognitive subtypes of schizophrenia may be associated with distinct differences in connectivity in the triple-network model. This categorization may foster further analysis of the effects of therapy on these network connectivity patterns, which may help to guide therapeutic choices to effectively reach personalized treatment goals.

Neuropsychopharmacology (2021) 46:1502–1509; https://doi.org/10.1038/s41386-020-00926-y

INTRODUCTION

Schizophrenia is a complex mental disorder associated with aberrant intrinsic functional coupling between large-scale neurocognitive networks, especially the brain triple-network model, which includes the default-mode network (DMN), central executive network (CEN), and salience network (SN) [1–4]. Prior evidence has indicated aberrant interactions of the DMN and CEN with the anterior insula aspect of the SN in schizophrenia [5]. Based on that observation, it is possible that heterogeneous symptom presentations in schizophrenia, including varying positive and negative symptoms and cognitive deficits, may be related to abnormal switching between the DMN and CEN related to functional dysconnectivity with the SN [6–8]. Additionally, enhanced interconnectivity between the CEN and DMN may underlie reality distortions and cognitive processing deficits, which may lead to a rise in psychotic perceptions of individuals at high risk for psychosis [3]. In this context, during working memory tasks, patients with schizophrenia exhibited abnormal activation in nodes of the SN and CEN, in contrast to DMN deactivation [4]. Moreover, neuroanatomical evidence has suggested that reduced surface area of this brain triple-network model (principally the SN and DMN) may be associated with symptom burden in patients with schizophrenia [9]. Exploration of aberrant connectivity patterns in this triple-network model offers a powerful approach to discover brain network-level alterations that may contribute to identifying features of schizophrenia [1, 2, 10]. In light of these findings, aberrant brain triple-network connectivity could constitute a clinically relevant neurobiological marker that may contribute to our understanding of the psychopathological underpinnings of schizophrenia.

Schizophrenia is clinically and biologically heterogeneous which has impeded the study of the disorder [11]. Increasing numbers of studies have applied machine learning algorithms to characterize the heterogeneity of schizophrenia in the search for subgroup distinctions that may enable personalized treatment and prognostic outcomes [12–18]. The neuroanatomic subtype of schizophrenia patients with pervasive brain gray matter loss has a longer illness duration and poorer premorbid functioning than those

[1]Mental Health Center & Psychiatric Laboratory, State Key Laboratory of Biotherapy, West China Hospital, Sichuan University, 610041 Chengdu, Sichuan, China; [2]West China Brain Research Centre, West China Hospital, Sichuan University, 610041 Chengdu, Sichuan, China; [3]Department of Psychiatry, University of Alberta, Edmonton, AB T6G 2B7, Canada; [4]Suzhou Psychiatry Hospital, Affiliated Guangji Hospital of Soochow University, 215137 Suzhou, Jiangsu, China; [5]CAS Key Laboratory of Behavioral Science, Institute of Psychology, 100101 Beijing, China and [6]Department of Psychology, University of Chinese Academy of Sciences, 100101 Beijing, China
Correspondence: Tao Li (litaohx@scu.edu.cn)

Received: 23 June 2020 Revised: 7 November 2020 Accepted: 12 November 2020
Published online: 6 January 2021

without such loss [13, 14]. Additionally, two distinct schizophrenia subgroups identified by measures of cognition and electrophysiology had different responses to dopaminergic blockade by antipsychotics [15]. Dysconnectivity of the brain mirror and mentalizing networks was also used to identify subtypes of schizophrenia accompanied by different cognitive abilities and functional outcomes [16]. Recent studies have indicated that the brain triple-network model as a distinctive marker can be used to distinguish schizophrenia from psychotic bipolar disorder or major depression, which could be helpful in clarifying the pathophysiology underlying discrete prognostic groups [2, 6, 19]. Based on SN-centered connectivity patterns, promising performance has been achieved with a range of accuracy from 78 to 80% in differentiating patients with schizophrenia from healthy controls (HCs) [6]. It should be noted that dysfunction in large-scale brain networks may give rise to specific symptoms of mental disorders, and subtyping dysfunction in this way may allow us to account for the natural heterogeneity of at least some psychiatric disorders [20]. Few studies have yet attempted to investigate the subtypes of schizophrenia in relation to differing connectivity patterns in the brain triple-network model.

In the present study, we hypothesized that neurobiological variance in characteristics of the brain triple-network model could define distinct types of the disorder within diagnostic boundaries. We conducted a data-driven, brain measure-based clustering approach to analyze resting-state functional connections (FCs) between key nodes of the triple-network model in patients with antipsychotic-naive first-episode schizophrenia (FES), to identify subtypes with specific brain circuit patterns. We validated the triple-network-pattern-based FES subgroups in an independent cohort. We also assessed the neurocognitive functions of patients with FES and HCs to investigate whether the distinct cognitive features were associated with potential brain-pattern-based subtypes of schizophrenia. We reevaluated and compared the clinical variables between patient subgroups at a 6-week follow-up to examine subgroup-specific differences following short-term antipsychotic treatment. Clarifying the heterogeneity in schizophrenia from a brain network-level perspective to identify biologically distinct subgroups may enhance our understanding of the psychopathology of schizophrenia and may be potentially helpful to achieve our goal of developing individualized treatment strategies for patients.

MATERIALS AND METHODS

Participants

Three hundred patients with FES and 301 HCs were included in this study. The discovery dataset (134 patients and 134 controls) was acquired with a Signa 3.0 Tesla (T) scanner (EXCITE, General Electric, USA) and used to select features and identify potential brain triple-network-pattern-based subgroups of FES. The replication dataset (166 patients and 167 controls) was acquired on a Philips 3.0 T (Achieva, TX, Best, Netherlands) scanner and used to validate the FES subgroups. Age and sex were matched between patients and HCs in each dataset. All participants were right-handed Chinese. The demographic characteristics of the participants in the discovery and replication datasets are displayed in Table S1. The severity of symptoms was assessed using the Positive and Negative Syndrome Scale (PANSS) [21]. The severity of illness was assessed using the global assessment of functioning scale (GAF). See details in the Supplementary Information. At the baseline assessment, neurocognitive function of the patients with FES and HCs was evaluated by using the short version of the Wechsler Adult Intelligence Scale—revised in China (WAIS-RC) and the computerized Cambridge Neurocognitive Test Automated Battery (CANTAB) as we have previously reported [22]. The neurocognitive tasks and measurements are briefly described in Table S2.

In the discovery dataset, a subset of individuals had data available at 6 weeks. At the 6-week follow-up assessment, 49 patients were reevaluated using the PANSS. Side effects of second-generation antipsychotics were assessed via the Treatment Emergent Symptom Scale (TESS), and antipsychotic medication exposure was expressed in chlorpromazine equivalents [23]. This study was approved by the ethics committee of West China Hospital, Sichuan University, in accordance with the Declaration of Helsinki, and all participants provided a priori written informed consent.

Image acquisition and data preprocessing

Resting-state functional magnetic resonance imaging (fMRI) and high-resolution T1 imaging data were acquired from each participant. Scanning parameters are listed in the Supplementary information.

Neuroimaging data were processed using FSL tools (FMRIB's Software Library) [24]. fMRI volumes were registered to the individual's structural scan and standard space images using FMRIB's Linear Image Registration Tool. Subjects with framewise displacement values larger than 0.3 mm were excluded from all analyses [25]. After quality control, the discovery and replication datasets had 127 controls and 130 patients, and 162 controls and 156 patients, respectively.

Seed-based analysis for the brain triple-network model

After preprocessing, Nilearn (https://nilearn.github.io/) was implemented to create masks and extract time series in 6-mm radius spheres around coordinates of eight nodes in this brain triple-network model as defined in prior studies (see Table S3) [2, 26]. The brain nodes included the ventromedial prefrontal cortex (vMPFC), posterior cingulate cortex (PCC), bilateral fronto-insular cortex (FIC), anterior cingulate cortex (ACC), dorsolateral prefrontal cortex (DLPFC), and bilateral posterior parietal cortex (PPC). At the individual level, Fisher's *r*-to-*z* transformation was conducted to compute the temporal correlation coefficients between the brain regions prior to further analyses.

Cluster analysis

Feature selection. Two-sample t-tests were used to identify distinct FCs that discriminated the patients with FES from HCs. Using a relatively loose threshold of $P_{uncorr} < 0.05$, 15 FCs with significant differences were retained. The selected FCs are shown in Table S4. The flowchart in Fig. S1 illustrates the data analysis strategy for this study.

Unsupervised machine learning algorithms. Using the identified FCs representing the brain triple-network model, spectral clustering was conducted for class formation. The algorithm is computationally efficient and works well for a small number of clusters [27]. It often outperforms traditional clustering methods such as *k*-means. To estimate clustering validity, we used the Calinski–Harabasz (CH) score and silhouette score to identify the most reliable cluster number [28, 29]. These validity measures are used in combination with the Euclidean distance, leading to a strong preference for spherical clustering [30]. Finally, dimensionality reduction techniques, including principal component analysis (PCA) and *t*-distributed stochastic neighbor embedding (t-SNE), were used to visualize the clustering of patient subgroups.

Independent dataset validation. To estimate the robustness of brain-pattern-based FES subgroups defined in the discovery dataset, identified FCs of the brain triple-network model were extracted from the replication dataset—an independent (unseen) cohort. We then applied cluster analysis and cluster validation as described above to the replication dataset to investigate patient subgroups with distinct triple-network patterns. We also computed the correlations across connectivity values, averaged

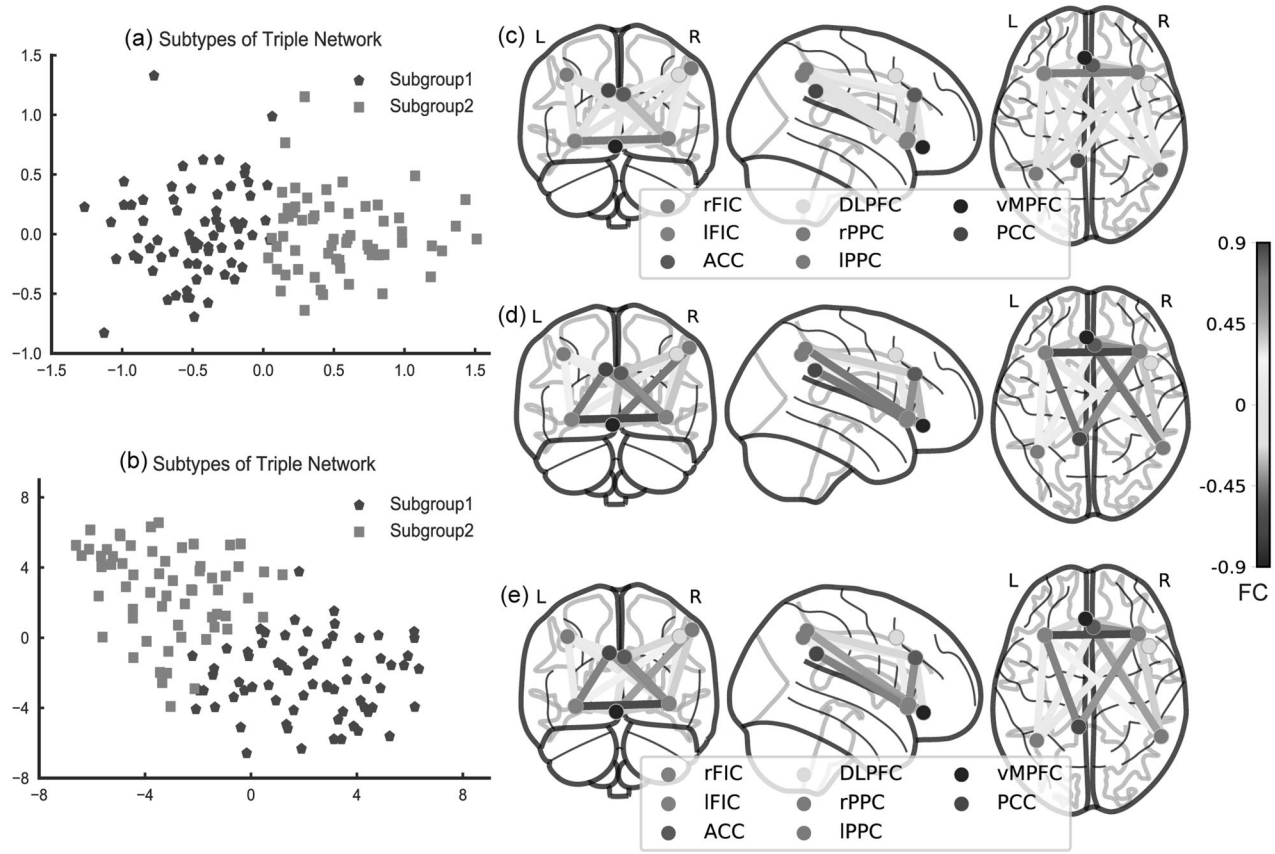

Fig. 1 Triple-network pattern-based FES subgroups in the discovery dataset. a Clusters are plotted using PCA in the discovery dataset. Two-dimensional principal subspace for patient subgroups. The *X*-axis represents the value of the first principal component that accounts for the largest possible variance in the dataset. The *Y*-axis represents the value of the second principal component. **b** Clusters are plotted using t-SNE. Two-dimensional embedded subspace for patient subgroups. The *X*-axis represents the value of the first embedded space by t-SNE. The *Y*-axis represents the value of the second embedded space. **c** Subgroup 1. **d** Subgroup 2. **e** Healthy controls. L left, R, right. The colorbar represents FC values. ACC anterior cingulate cortex, FIC fronto-insular cortex, DLPFC dorsolateral prefrontal cortex, PPC posterior parietal cortex, vMPFC ventromedial prefrontal cortex, PCC posterior cingulate cortex.

across subjects, between-patient subgroups in the discovery and replication datasets.

Statistical significance of clustering. We used a SigClust approach to assess the significance of clustering [31]. Here, we applied the R package *SigClust* to compute the empirical *P*-value and Gaussian fit *P*-value to test the statistical significance. We also tested the significance of clustering using the bootstrapping method. See Supplementary Information for more details.

Statistical analysis

We compared demographic characteristics between patient subgroups and HCs using analysis of variance (ANOVA) for continuous variables and χ^2 tests for categorical variables (sex, marriage status, and family history). Nonparametric Mann–Whitney *U* tests were used to compare the duration of illness (DUI) between patient subgroups. Baseline differences in clinical symptom severity (PANSS total scores and PANSS subscale scores) between patient subgroups were estimated using analysis of covariance with DUI as a covariate. Two-sample *t*-tests were used to compare GAF scores, follow-up reassessed PANSS scores, and reduction in PANSS total scores [32]. ANOVA was used to compare intelligence quotient (IQ) scores, and nonparametric Kruskal–Wallis tests were applied to analyze cognitive variables from the tasks in the CANTAB between patient subgroups and HCs. All statistical test results were considered significant with false discovery rate (FDR) correction: $P_{FDR} < 0.05$. Effect size (ES) and statistical power were calculated for PANSS scores and FCs between patient subgroups.

RESULTS

FES subgroups with differing triple-network patterns identified in discovery dataset

In the discovery dataset, based on the selected FCs of the brain triple-network model, when the optimal cluster number was equal to two, the cluster results yielded the maximum CH score and maximum silhouette score (see Fig. S2a, b). The results of the SigClust and bootstrapping methods indicated that the two subgroups represented the most appropriate data structure (see Figs. S3a and S4). Clustering subgroups were also visualized by PCA and t-SNE (see Fig. 1a, b). Subsequent analyses mainly focused on these two patient subgroups with different triple-network patterns. In the discovery dataset, subgroup 1 had 69 patients (53.08%) and subgroup 2 had 61 patients (46.92%). Relative to the HC group, subgroup 1 was characterized by SN-centered decreased FCs between key nodes of the triple-network model, while subgroup 2 exhibited relatively increased FCs, especially between the vMPFC, ACC, and right PPC (see Fig. 2a, b). Compared to subgroup 1, subgroup 2 showed SN-centered hyperconnectivity that was dominant between nodes of the brain triple-network model (see Fig. 1c–e and Table S5). The ES and statistical power of the FCs for the patient subgroups versus the HC group are described in Table S6.

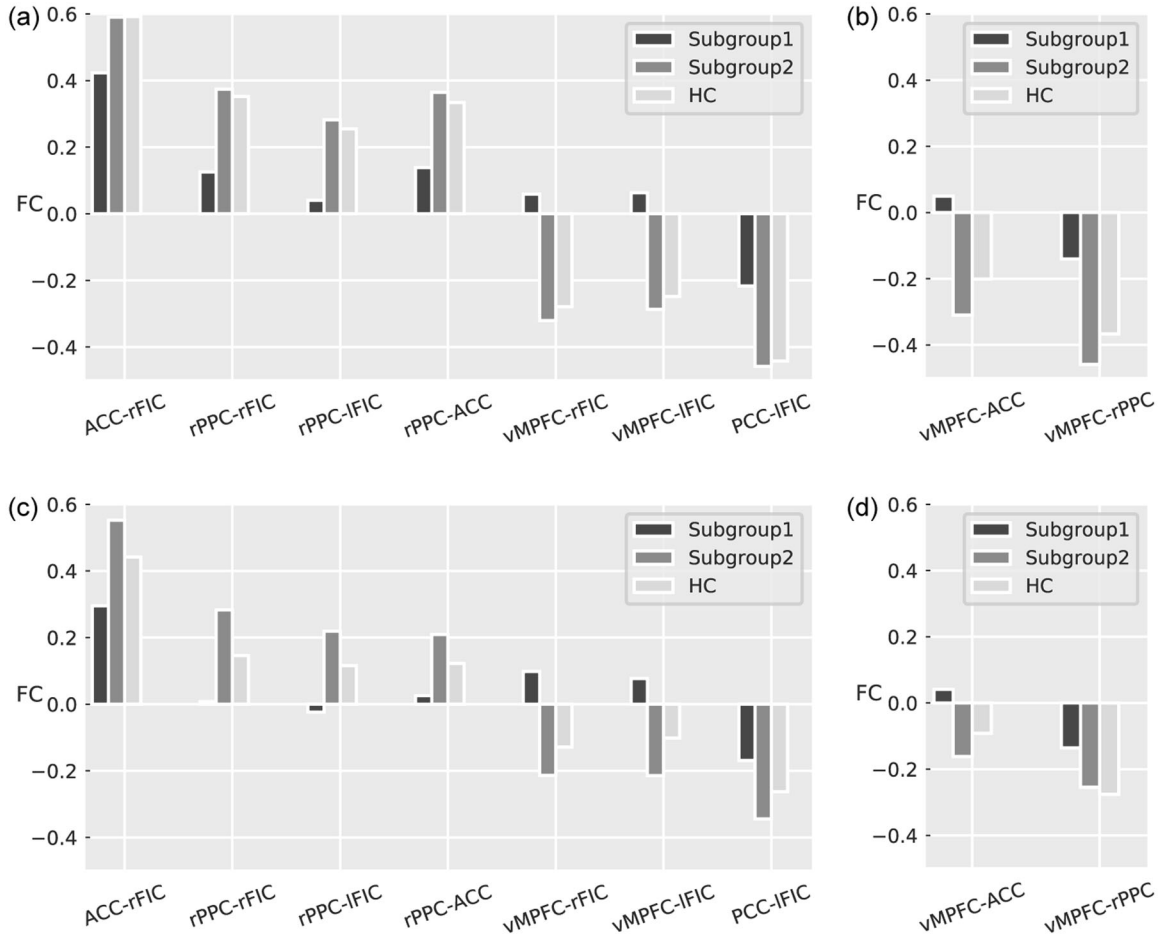

Fig. 2 FCs between the FES subgroups and HC group in discovery and replication datasets. a FDR-corrected FCs among patient subgroups and the HC group in the discovery dataset. **b** FDR-corrected FCs between each pair of groups (subgroup 1, subgroup 2 and HC) in the discovery dataset. **c** FDR-corrected FCs between each pair of groups (subgroup 1, subgroup 2 and HC) in the replication dataset. **d** FDR-corrected FCs among patient subgroups and the HC group in the replication dataset. L left, R right, ACC anterior cingulate cortex, FIC fronto-insular cortex, DLPFC dorsolateral prefrontal cortex, PPC posterior parietal cortex, vMPFC ventromedial prefrontal cortex, PCC posterior cingulate cortex.

Although not significant at the FDR-corrected level, subgroup 1 tended to suffer more severe clinical symptoms with higher PANSS total scores (ES = 0.29, power = 0.39) and scores on the PANSS general psychopathology scale (ES = 0.36, power = 0.56) than subgroup 2. No significant differences were observed in demographic and clinical variables between patient subgroups (see Table 1).

Both patient subgroups had lower IQ and worse performance in the cognitive tasks than the HC group. Subgroup 1 had more false alarms in block 5 of the Rapid Visual Information Processing (RVP) task than the HC group ($H_{2,\ 121} = -3.41$, $P_{FDR} = 0.006$), which suggested that subgroup 1 had greater deficits in sustained attention and information processing. Subgroup 2 had more errors in block 7 of the Intra/Extra-Dimensional Set Shift (IED) task than the HC group ($H_{2,\ 116} = -3.14$, $P_{FDR} = 0.006$), which indicated that subgroup 2 had greater impairments in cognitive flexibility and shifting. In contrast to the patient subgroup versus HC group comparisons, no significant differences were found between the patient subgroups across all neurocognitive tests (see Table S7).

Triple-network-pattern-based FES subtypes validated in the replication dataset

In the replication dataset, using selected FCs of the brain triple-network model, a cluster number of two achieved the maximum CH score and silhouette score (see Fig. S2c, d). The results of the SigClust and bootstrapping methods suggested that the two subgroups were the best fit for the underlying data structure (see Figs. S3b and S5). Patient subgroups with different brain triple-network patterns were also visualized by PCA and t-SNE (see Fig. S6a, b). In the replication dataset, 75 patients (48.08%) were placed in subgroup 1 and 81 patients (51.92%) were placed in subgroup 2. Using the FCs within the triple-network model identified in the discovery dataset, the patient subgroups were validated in the replication dataset—subgroup 1 was characterized by SN-centered hypoconnectivity within the triple-network model and subgroup 2 was marked by increased connectivity, especially connectivity between the vMPFC, ACC, right PPC, and bilateral FIC (see Fig. 2c, d, Fig. S6 and Table S8). The ES and statistical power of the FCs for the patient subgroups versus the HC group in the replication dataset are listed in Table S9.

In the replication dataset, subgroup 1 tended to experience higher PANSS total scores (ES = 0.20, power = 0.23), positive scale scores (ES = 0.20, power = 0.23), and negative scale scores (ES = 0.20, power = 0.23) than subgroup 2. However, there were no statistically significant differences between patient subgroups in demographic and clinical variables (see Table S10).

Similar neurocognitive results between the patient subgroups and the HC group were found in the replication dataset (see Table S11). Subgroup 1 had more false alarms in block 5 of the RVP task ($H_{2,\ 228} = -2.91$, $P_{FDR} = 0.012$), while subgroup 2 had more errors in block 7 of the IED task ($H_{2,\ 221} = -2.50$, $P_{FDR} = 0.036$) than the HC group. Again, no evident differences were

Table 1. Demographic and clinical characteristics of discovery dataset and longitudinal subset.

	Discovery dataset				Longitudinal subset baseline			6-week follow-up		
	HC ($n = 127$)	Subgroup 1 ($n = 69$)	Subgroup 2 ($n = 61$)	$F/T/\chi^2$	Subgroup 1 ($n = 27$)	Subgroup 2 ($n = 22$)	T/χ^2	Subgroup 1 ($n = 27$)	Subgroup 2 ($n = 22$)	T
Age (years)	25.72 (7.82)	24.25 (8.11)	24.85 (7.86)	0.82	23.15 (6.80)	24.18 (8.62)	−0.47	–	–	–
Sex (M/F)	58/69	31/38	29/32	0.10	11/16	11/11	0.42	–	–	–
Education (years)	13.43 (3.34)	12.07 (2.73)	12.23 (3.39)	5.12*	12.15 (3.28)	12.64 (2.61)	−0.57	–	–	–
Marital status (married/unmarried)	35/89	14/55	16/42	1.57	5/22	5/17	0.13	–	–	–
Family history (Yes/No)	–	21/48	13/47	1.27	11/13	9/13	0.11	–	–	–
GAF scores	–	27.72 (9.57)	28.85 (9.86)	−0.63	26.42 (6.94)	29.05 (9.17)	−1.11	56.32 (15.13)	54.95 (15.91)	0.29
DUI (months)	–	2	3	1.19	2	5.5	1.22	–	–	–
Medication	–	–	–	–	–	–	–	284.55 (129.58)	318.10 (144.48)	−0.64
TESS	–	–	–	–	–	–	–	2.00	2.50	−0.21
PANSS-TS	–	93.02 (16.69)	87.02 (20.74)	2.92	98.04 (14.06)	90.55 (15.59)	1.81	67.92 (19.35)	63.32 (19.03)	0.79
PANSS-P	–	24.91 (7.24)	24.55 (6.83)	0.05	26.92 (7.65)	26.85 (5.26)	0.22	13.24 (4.44)	14.63 (4.46)	−1.03
PANSS-N	–	19.80 (7.12)	17.93 (9.62)	3.10	20.31 (5.88)	16.15 (7.88)	3.69	17.44 (6.75)	13.42 (5.19)	**2.15***
PANSS-GP	–	48.31 (9.50)	44.54 (9.95)	3.74	50.81 (8.23)	47.55 (7.69)	1.30	34.48 (9.77)	32.63 (9.66)	0.63
PANSS Reduction %	–	–	–	–	–	–	–	0.29 (0.15)	0.28 (0.14)	0.26

PANSS Positive and Negative Syndrome Scale, *PANSS-TS* PANSS total score, *PANSS-P* PANSS - positive subscale, *PANSS-N* PANSS - negative subscale, *PANSS-GP* PANSS - psychopathological symptoms, *GAF* Global Assessment of Functioning Scale, *TESS* Treatment Emergent Symptom Scale, *DUI* duration of illness, *M* male, *F* female. Mean (standard deviation). Medication, chlorpromazine equivalents (mg/day). *$P_{uncorr} < 0.05$.
At the 6-week follow-up, subgroup 1 tended to have higher score of PANSS-N than subgroup 2 ($T = 2.15$, $P_{uncorr} = 0.037$).

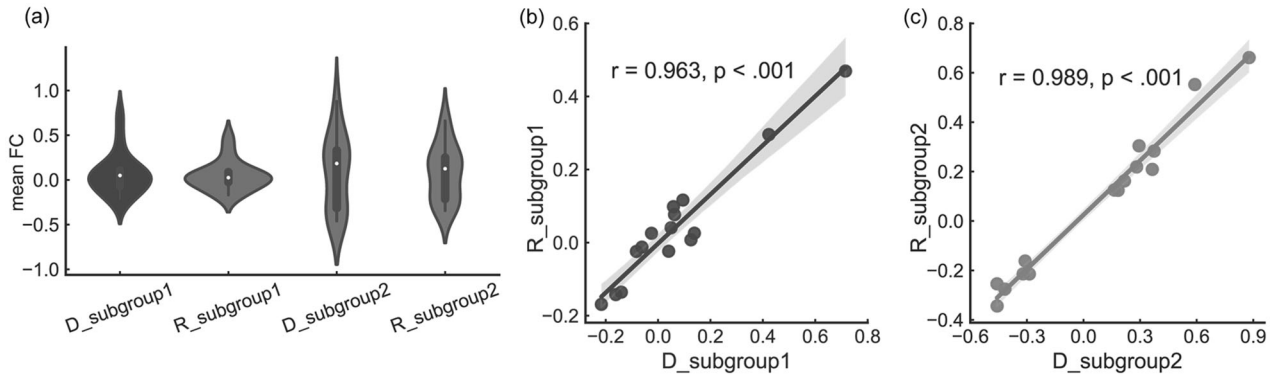

Fig. 3 Triple-network-based FES subgroups in discovery and replication datasets. a In the violin plot, the *Y*-axis represents the mean FC values and the *X*-axis represents subgroups in the discovery dataset and replication datasets. D for the discovery dataset. R for the replication dataset. **b** Pearson correlation between subgroup 1 in the discovery and replication datasets. **c** Pearson correlation between subgroup 2 in these two datasets.

found between the patient subgroups across all neurocognitive tests, even though we ruled out possible causes, such as the presence of outliers, or the method of statistical analysis (see Supplementary Results and Figs. S7–9).

Based on the mean FC values, a violin plot was used to display the distribution for each subgroup and its probability density (Fig. 3a). Using the mean FC values, subgroup 1 in the discovery dataset was highly correlated with subgroup 1 in the replication dataset ($r = 0.963$, $P_{FDR} < 0.001$). Subgroup 2 in the discovery and replication dataset was highly correlated ($r = 0.989$, $P_{FDR} < 0.001$) (see Fig. 3b, c).

Triple-network-pattern-based FES subtypes in the longitudinal subset

In the longitudinal subset of the discovery dataset, subgroup 1 had 27 patients and subgroup 2 had 22 patients. Table S12 describes the FCs within the brain triple-network model between these patient subgroups. Compared to subgroup 2, subgroup 1 exhibited SN-centered decreased connectivity within the brain triple-network model (see Fig. 4 and Table S12). At the baseline assessment of the longitudinal subset with DUI as a covariate, subgroup 1 had higher scores on the PANSS negative scale (ES = 0.63, power = 0.62) and general psychopathology scale (ES = 0.42, power = 0.33) than subgroup 2 (see Table 1). At the 6-week follow-up, subgroup 1 tended to have more serious negative symptoms than subgroup 2 ($P_{uncorr} = 0.037$, ES = 0.69, power = 0.71). However, no significant differences were observed between the patient subgroups in demographic and clinical variables.

DISCUSSION

In the present study, we used both hypothesis- and data-driven approaches to different datasets and identified two FES subtypes

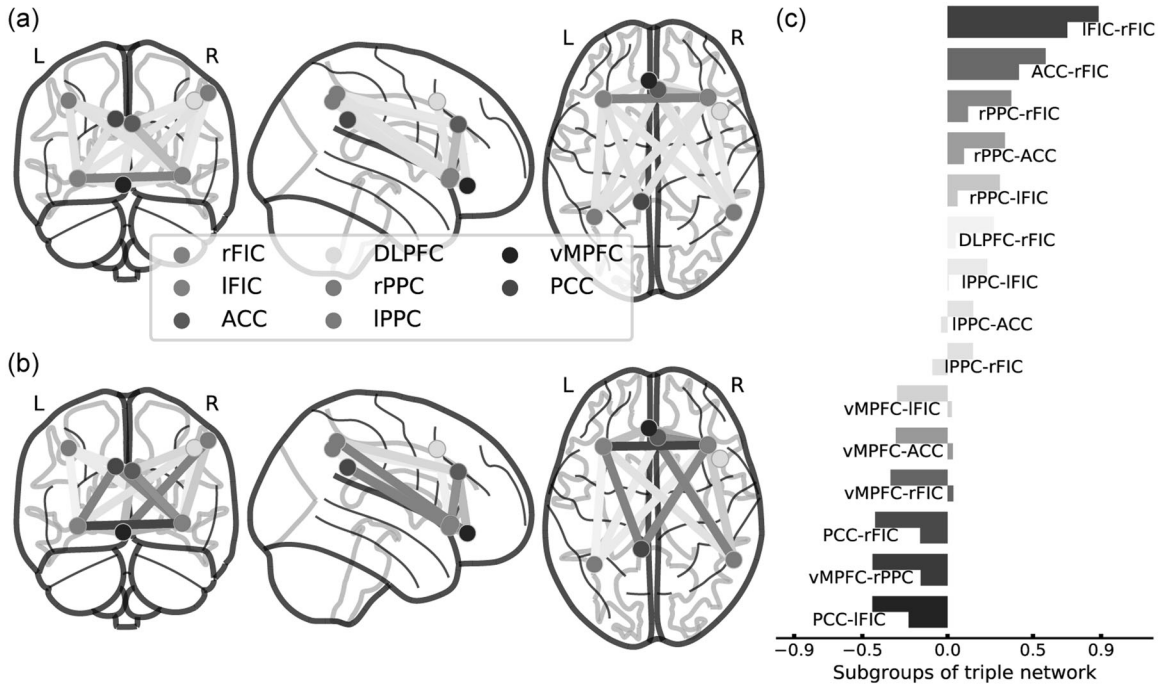

Fig. 4 Triple-network-pattern-based FES subgroups in the longitudinal dataset. a Subgroup 1. **b** Subgroup 2. **c** Comparisons of FCs between patient subgroups. In horizontal bars with the same color, the upper bar represents subgroup 1 and the lower bar represents subgroup 2. The *X*-axis represents FC values. L left, R right, ACC anterior cingulate cortex, FIC fronto-insular cortex, DLPFC dorsolateral prefrontal cortex, PPC posterior parietal cortex, vMPFC ventromedial prefrontal cortex, PCC posterior cingulate cortex.

with differing resting-state connectivity profiles in relation to the brain triple-network model. Our current findings extend our knowledge about subtypes of schizophrenia through a brain network-level perspective. Compared to the HC group, one patient subgroup was characterized by SN-centered decreased connectivity within the triple-network system, exhibited greater deficits in sustained attention and appeared to have a more severe symptom burden. In contrast, the subgroup with hyper-connectivity of key nodes in the triple-network model experienced greater deficits in cognitive flexibility. Subtypes of schizophrenia with differing brain triple-network patterns and neurocognitive features were validated in an independent cohort. In the longitudinal subset of the discovery dataset, at the 6-week follow-up, the subgroup with SN-centered hypoconnectivity within the triple-network model tended to have more severe and persistent negative symptoms (with a medium effect size) than the patient subgroup with hyperconnectivity. This study provides evidence to support the hypothesis that biologically and clinically relevant subtypes of FES exist with differing brain triple-network patterns in the early stage of the disorder.

Consistent with prior research, the findings of the current study confirmed that patients with schizophrenia were characterized by altered connectivity in core large-scale neurocognitive networks [1–3, 5]. The functionally disengaged interaction of the SN with the CEN and DMN could be a distinct signature of brain network-level dysfunction in schizophrenia [6, 33]. Notably, in this study, the patient subgroup with SN-centered hypoconnectivity within the triple-network model at baseline appeared to be associated with more persistent negative symptoms even after short-term antipsychotic treatment in the early course of schizophrenia. Longitudinal studies are needed to investigate the long-term therapeutic efficacy and prognosis for patients with different schizophrenia subtypes. This observation is interesting in relation to evidence suggesting that atypical antipsychotics may regulate DMN connectivity through reduced connectivity in the PCC and increased connectivity in the vMPFC in early-phase schizophrenia [34, 35]. Patients with FES exposed to short-term antipsychotic treatment may exhibit increased synchronous regional brain function in insular and frontal-temporal areas and reduced connectivity in temporal-parietal areas and in the network between regions of the DMN and medial frontal areas [36]. Dysconnectivity with this brain triple-network model could be a significant neuroimaging biomarker for tracking antipsychotic effects in patients with schizophrenia. Additionally, it is notable that a brain network-level perspective may be useful, in comparison to a focus on neurotransmitter systems per se, to model or explain the effects of antipsychotics on brain function in schizophrenia [37]. From this perspective, our current findings may provide new insights into the actions of antipsychotic treatment in patients with varying subtypes of schizophrenia in relation to differing brain circuit patterns.

In accordance with prior research [8], this study also indicated that the subgroup of schizophrenia patients with SN-centered hypoconnectivity within the triple-network system tended to have more severe negative symptoms. Additionally, a subgroup of schizophrenia patients characterized by global gray matter volume reduction (including insular cortex, medial prefrontal cortex, and other brain areas) was associated with longer illness duration and poorer premorbid functioning [13, 14]. Subtypes of FES characterized by pervasive disrupted white matter patterns appeared to have greater negative symptoms [12]. Moreover, patients with deficit schizophrenia enduring persistent negative symptoms had poorer cognitive performance and broader impaired functional segregation in brain networks than those with nondeficit schizophrenia [38]. Patients with treatment-resistant schizophrenia, as a complex neurobiological category, exhibited frontal gray matter reduction, decreased fiber tract integrity and widespread resting-state hypoconnectivity especially in frontal, temporal, and occipital regions [39, 40]. Similarities in functional and structural neuroimaging studies probably hint that subtypes of schizophrenia with more prominent reductions in brain measures are likely to correspond to greater clinical

symptom burden and poorer therapeutic outcome. Subtypes of schizophrenia with differing brain alterations may imply that these neurobiological substrates could be the key sources of disorder heterogeneity. Meanwhile, subtypes of patients with schizophrenia with distinct brain abnormalities may reflect qualitatively distinct genetic factor influences or altered neurodevelopment in the early-stage and long-term illness trajectories [12–14, 18]. Parsing the neurobiological heterogeneity of schizophrenia could be useful to determine the more severe subtypes and improve accuracy in treatment selection. Whether individuals with deficit type or treatment-resistant schizophrenia will be clustered to the subtype with widespread brain alterations needs future longitudinal studies to examine.

Schizophrenia is associated with broad neurocognitive deficits [4, 5, 41]. Consistent with previous studies, the present study also found that each schizophrenia subgroup had specific cognitive impairments compared to controls. However, with a limited sample size in the same cohort, there may not have been enough power to use cognitive features to directly distinguish one patient subgroup from the other. In this study, patient subgroup 2 seemed to have similar brain connectivity patterns to those of controls, with the exception of hyperconnectivity between the vMPFC, ACC, and PPC. Notably, the subtype of schizophrenia marked by increased connectivity within the triple-network model (especially the DMN and CEN) tended to have more impairments in cognitive flexibility. A prior study reported that hyperconnectivity of the DMN and CEN was adversely related to cognitive performance in individuals with an at risk mental state for psychosis [3]. Likewise, enhanced interconnectivity of the DMN and CEN was positively correlated with severity of psychotic symptoms in patients with schizophrenia during the acute psychotic episode and even during a remission period [5, 8]. Higher resting-state dynamic connectivity between the CEN and DMN was also associated with poorer cognitive flexibility in healthy control individuals [42]. Additionally, aberrant hypodeactivation in the DMN in schizophrenia could be caused by a reduction in the influence of the insula during cognitive tasks [4]. Dysfunction in the DMN may be a source of general cognitive impairment, especially cognitive flexibility deficits for patients with schizophrenia [7, 43]. Our current results also indicate that schizophrenia subgroups with different dysfunctional connectivity between the CEN and DMN might be associated with correlated impairments in cognitive flexibility.

Concurrently, the subgroup of schizophrenia patients with SN-centered hypoconnectivity within the triple-network model had greater deficits in sustained attention and information processing. Increasing evidence suggests that an aberrant or attenuated interconnection between the SN and the CEN and DMN may contribute to the genesis of psychotic symptoms and cognitive deficits, especially attentional impairments in schizophrenia [3, 6–8, 44]. Additionally, inflammatory processes may also contribute to cognitive deficits in schizophrenia, as a subgroup of patients with schizophrenia with higher plasma cytokine levels and kynurenine/tryptophan ratio has been shown to have greater attentional impairment and reduced gray matter volume in the DLPFC [17]. Moreover, rare variants in the signaling of the zinc transporter gene have been associated with a subtype of psychosis with severe negative symptoms and global cognitive impairments [18]. These findings may help to elucidate neural, inflammatory, and genetic mechanisms associated with subtypes of schizophrenia with differing brain circuits and cognitive impairments.

Several limitations should be considered. First, the longitudinal subset sample size was relatively small and future longitudinal studies with larger sample sizes and long-term follow-up will be necessary to confirm the current findings and further exploit brain triple-network-based biotypes of schizophrenia. Second, some clinical information, including early life stress, cigarette smoking, and comorbid conditions (depressive symptoms and obsessional traits), was not fully recorded for each patient. These data are important as a prior study suggested that cigarette smoking could influence interactions between this brain triple-network system [45]; additional clinical information will be helpful in future studies. Third, our patient subgroups did not exhibit statistically significant differences among our clinical and neurocognitive variables, in contrast to the patient subgroup versus HC group comparisons. This issue needs to be studied further in future studies with larger and independent samples. Future studies should also focus on a more fine-grained set of clinical features to better characterize differences between patient subgroups with differing triple-network-pattern profiles. Fourth, using univariate selection, less redundant and more distinct features were identified to further investigate the brain patterns underlying the data structure, yet this approach might have overlooked the group-level heterogeneity of functional connectivity in the disorder. This should be considered in future studies.

CONCLUSIONS

Our findings support the presence of two neurobiologically distinct subtypes of schizophrenia based on brain triple-network patterns, accompanied by distinct deficits in sustained attention and cognitive flexibility and probably different symptom burdens. Patients identified as fitting the subtype of schizophrenia marked by SN-centered hypoconnectivity within the triple-network model will likely have more persistent negative symptoms, an observation that may allow more precise treatment selections and improved prognosis. Parsing the heterogeneity of schizophrenia, from a functional network-based perspective, may potentially facilitate the development of effective individualized treatment strategies.

FUNDING AND DISCLOSURE

This work was supported by the National Natural Science Foundation of China Key Project (81630030 and 81920108018 to T.L.); the National Key Research and Development Program of the Ministry of Science and Technology of China (2016YFC0904300 to T.L.); the 1.3.5 Project for disciplines of excellence, West China Hospital of Sichuan University (ZY2016103, ZY2016203 and ZYGD20004 to T.L.); the National Natural Science Foundation of China (grant number 81801326 to S.L.; grant number 81571320 to W.D.); the Introduction Project of Suzhou Clinical Expert Team (SZYJTD201715 to X.D. and T.L.). The authors have declared that there are no conflicts of interest in relation to the subject of this study.

ACKNOWLEDGEMENTS

We warmly thank Professor Nan-kuei Chen (Radiology Medical Research Lab, University of Arizona) for helping with the fMRI preprocessing analysis. We also warmly thank all the participants for their participation in the study.

AUTHOR CONTRIBUTIONS

All authors have made significant scientific contributions to this manuscript. T.L., W.D., and X.M. designed the study and wrote the protocol. S.L., Q.W., and X.L. managed the literature searches and analyses. H.R., C.Z., M.L., and Y.M. conducted interviews with participants. H.Y., W.W., Y.M., and L.Z. gathered the data. S.L. undertook the statistical analysis with some help from C.-G.Y., Q.W., and A.J.G., and S.L. wrote the first draft of the manuscript. A.J.G., T.L., X.D., and C.-G.Y. were involved in the revision and completion of the work. All authors contributed to and approved the final manuscript.

ADDITIONAL INFORMATION

Supplementary Information accompanies this paper at (https://doi.org/10.1038/s41386-020-00926-y).

Publisher's note Springer Nature remains neutral with regard to jurisdictional claims in published maps and institutional affiliations.

REFERENCES

1. Menon V. Large-scale brain networks and psychopathology: a unifying triple network model. Trends Cogn. Sci. 2011;15:483–506.
2. Palaniyappan L, Deshpande G, Lanka P, Rangaprakash D, Iwabuchi S, Francis S, et al. Effective connectivity within a triple network brain system discriminates schizophrenia spectrum disorders from psychotic bipolar disorder at the single-subject level. Schizophr. Res. 2019;214:24–33.
3. Wotruba D, Michels L, Buechler R, Metzler S, Theodoridou A, Gerstenberg M, et al. Aberrant coupling within and across the default mode, task-positive, and salience network in subjects at risk for psychosis. Schizophr. Bull. 2014;40:1095–104.
4. Wu, D. & Jiang, T. Schizophrenia-related abnormalities in the triple network: a meta-analysis of working memory studies. Brain Imaging Behav. 2019. https://doi.org/10.1007/s11682-019-00071-1.
5. Manoliu A, Riedl V, Zherdin A, Muhlau M, Schwerthoffer D, Scherr M, et al. Aberrant dependence of default mode/central executive network interactions on anterior insular salience network activity in schizophrenia. Schizophr Bull. 2014;40:428–37.
6. Supekar K, Cai W, Krishnadas R, Palaniyappan L, Menon V. Dysregulated brain dynamics in a triple-network saliency model of schizophrenia and its relation to psychosis. Biol Psychiatry. 2019;85:60–9.
7. Nekovarova T, Fajnerova I, Horacek J, Spaniel F. Bridging disparate symptoms of schizophrenia: a triple network dysfunction theory. Front Behav Neurosci. 2014;8:171.
8. Manoliu A, Riedl V, Doll A, Bauml JG, Muhlau M, Schwerthoffer D, et al. Insular dysfunction reflects altered between-network connectivity and severity of negative symptoms in schizophrenia during psychotic remission. Front Hum Neurosci. 2013;7:216.
9. Palaniyappan L, Mallikarjun P, Joseph V, White TP, Liddle PF. Regional contraction of brain surface area involves three large-scale networks in schizophrenia. Schizophr Res. 2011;129:163–8.
10. Gong Q, Hu X, Pettersson-Yeo W, Xu X, Lui S, Crossley N, et al. Network-level dysconnectivity in drug-naive first-episode psychosis: dissociating transdiagnostic and diagnosis-specific alterations. Neuropsychopharmacology 2017;42:933–40.
11. Tsuang MT, Lyons MJ, Faraone SV. Heterogeneity of schizophrenia. Conceptual models and analytic strategies. Br J Psychiatry. 1990;156:17–26.
12. Sun H, Lui S, Yao L, Deng W, Xiao Y, Zhang W, et al. Two patterns of white matter abnormalities in medication-naive patients with first-episode schizophrenia revealed by diffusion tensor imaging and cluster analysis. JAMA Psychiatry. 2015;72:678–86.
13. Dwyer DB, Cabral C, Kambeitz-Ilankovic L, Sanfelici R, Kambeitz J, Calhoun V, et al. Brain subtyping enhances the neuroanatomical discrimination of schizophrenia. Schizophr Bull. 2018;44:1060–69.
14. Chand GB, Dwyer DB, Erus G, Sotiras A, Varol E, Srinivasan D, et al. Two distinct neuroanatomical subtypes of schizophrenia revealed using machine learning. Brain 2020;143:1027–38.
15. Bak N, Ebdrup BH, Oranje B, Fagerlund B, Jensen MH, During SW, et al. Two subgroups of antipsychotic-naive, first-episode schizophrenia patients identified with a Gaussian mixture model on cognition and electrophysiology. Transl Psychiatry. 2017;7:e1087.
16. Viviano JD, Buchanan RW, Calarco N, Gold JM, Foussias G, Bhagwat N, et al. Resting-state connectivity biomarkers of cognitive performance and social function in individuals with schizophrenia spectrum disorder and healthy control subjects. Biol Psychiatry. 2018;84:665–74.
17. Kindler J, Lim CK, Weickert CS, Boerrigter D, Galletly C, Liu D, et al. Dysregulation of kynurenine metabolism is related to proinflammatory cytokines, attention, and prefrontal cortex volume in schizophrenia. Mol Psychiatry. 2019. https://doi.org/10.1038/s41380-019-0401-9.
18. Kranz TM, Berns A, Shields J, Rothman K, Walsh-Messinger J, Goetz RR, et al. Phenotypically distinct subtypes of psychosis accompany novel or rare variants in four different signaling genes. EBioMedicine 2016;6:206–14.
19. Han W, Sorg C, Zheng C, Yang Q, Zhang X, Ternblom A, et al. Low-rank network signatures in the triple network separate schizophrenia and major depressive disorder. NeuroImage Clin. 2019;22:101725.
20. Williams LM. Precision psychiatry: a neural circuit taxonomy for depression and anxiety. Lancet Psychiatry. 2016;3:472–80.
21. Kay SR, Flszbein A, Opfer LA. The positive and negative syndrome scale (PANSS) for schizophrenia. Schizophr Bull. 1987;13:261.
22. Liang S, Brown MRG, Deng W, Wang Q, Ma X, Li M, et al. Convergence and divergence of neurocognitive patterns in schizophrenia and depression. Schizophr Res. 2018;192:327–34.
23. Andreasen NC, Pressler M, Nopoulos P, Miller D, Ho BC. Antipsychotic dose equivalents and dose-years: a standardized method for comparing exposure to different drugs. Biol Psychiatry. 2010;67:255–62.
24. Jenkinson M, Beckmann CF, Behrens TE, Woolrich MW, Smith SM. FSL. NeuroImage. 2012;62:782–90.
25. Power JD, Barnes KA, Snyder AZ, Schlaggar BL, Petersen SE. Spurious but systematic correlations in functional connectivity MRI networks arise from subject motion. NeuroImage 2012;59:2142–54.
26. Sridharan D, Levitin DJ, Menon V. A critical role for the right fronto-insular cortex in switching between central-executive and default-mode networks. Proc Natl Acad Sci USA. 2008;105:12569–74.
27. Von Luxburg U. A tutorial on spectral clustering. Stat Comput. 2007;17:395–416.
28. Calinski T, Harabasz J. A dendrite method for cluster analysis. Commun Stat Theory Methods. 1974;3:1–27.
29. Rousseeuw PJ. Silhouettes: a graphical aid to the interpretation and validation of cluster analysis. J Comput Appl Math. 1987;20:53–65.
30. Van Craenendonck T, Blockeel H. Using internal validity measures to compare clustering algorithms. ICML [C]. Lille, France: 2015:1–8.
31. Liu Y, Hayes DN, Nobel A, Marron JS. Statistical significance of clustering for high-dimension, low–sample size data. J Am Stat Assoc. 2008;103:1281–93.
32. Leucht S. Measurements of response, remission, and recovery in schizophrenia and examples for their clinical application. J Clin Psychiatry. 2014;75:8–14.
33. Menon V, Uddin LQ. Saliency, switching, attention and control: a network model of insula function. Brain Struct Funct. 2010;214:655–67.
34. Sambataro F, Blasi G, Fazio L, Caforio G, Taurisano P, Romano R, et al. Treatment with olanzapine is associated with modulation of the default mode network in patients with Schizophrenia. Neuropsychopharmacology 2010;35:904–12.
35. Wang Y, Tang W, Fan X, Zhang J, Geng D, Jiang K, et al. Resting-state functional connectivity changes within the default mode network and the salience network after antipsychotic treatment in early-phase schizophrenia. Neuropsychiatr Dis Treat. 2017;13:397–406.
36. Lui S, Li T, Deng W, Jiang L, Wu Q, Tang H, et al. Short-term effects of antipsychotic treatment on cerebral function in drug-naive first-episode schizophrenia revealed by "resting state" functional magnetic resonance imaging. Arch Gen Psychiatry. 2010;67:783–92.
37. De Rossi P, Chiapponi C, Spalletta G. Brain functional effects of psychopharmacological treatments in schizophrenia: a network-based functional perspective beyond neurotransmitter systems. Curr Neuropharmacol. 2015;13:435–44.
38. Yu M, Dai Z, Tang X, Wang X, Zhang X, Sha W, et al. Convergence and divergence of brain network dysfunction in deficit and non-deficit schizophrenia. Schizophr Bull. 2017;43:1315–28.
39. Vita A, Minelli A, Barlati S, Deste G, Giacopuzzi E, Valsecchi P, et al. Treatment-resistant schizophrenia: genetic and neuroimaging correlates. Front Pharm. 2019;10:402.
40. Ganella EP, Bartholomeusz CF, Seguin C, Whittle S, Bousman C, Phassouliotis C, et al. Functional brain networks in treatment-resistant schizophrenia. Schizophr Res. 2017;184:73–81.
41. Dickinson D, Harvey PD. Systemic hypotheses for generalized cognitive deficits in schizophrenia: a new take on an old problem. Schizophr Bull. 2009;35:403–14.
42. Douw L, Wakeman DG, Tanaka N, Liu H, Stufflebeam SM. State-dependent variability of dynamic functional connectivity between frontoparietal and default networks relates to cognitive flexibility. Neuroscience 2016;339:12–21.
43. Vatansever D, Manktelow AE, Sahakian BJ, Menon DK, Stamatakis EA. Cognitive flexibility: a default network and basal ganglia connectivity perspective. Brain Connect. 2016;6:201–7.
44. Lefebvre S, Demeulemeester M, Leroy A, Delmaire C, Lopes R, Pins D, et al. Network dynamics during the different stages of hallucinations in schizophrenia. Hum Brain Mapp. 2016;37:2571–86.
45. Liao W, Fan YS, Yang S, Li J, Duan X, Cui Q, et al. Preservation effect: cigarette smoking acts on the dynamic of influences among unifying neuropsychiatric triple networks in schizophrenia. Schizophr Bull. 2019;45:1242–50.